Investigation of failure and damages on a continuous casting copper mould

Silvia Barella *, Andrea Gruttadauria, Carlo Mapelli, Davide Mombelli

Politecnico di Milano, Dipartimento di Meccanica, Via La Masa 1, 20156 Milano, Italy

Received 2 August 2013
Received in revised form 15 November 2013
Accepted 18 November 2013
Available online 27 November 2013

1. Introduction

Once the molten steel refining process is completed, the alloy contained in the ladle is usually sent to a continuous casting machine. The steel is poured from the ladle to a tundish and then from the tundish into a water-cooled copper mould that induces the formation of a thin, solidified steel shell (Fig. 1).

The main function of the mould is to produce and stabilize a solid shell resistant enough to contrast the metallic pressure of the liquid core and, thus, contain the liquid phase at the entry of the secondary spray cooling zone. If the mould system does not work properly, a break-out can take place and the hot liquid steel core can burst open, pouring liquid steel onto the machine and causing a very dangerous situation [1,2].

The mould is basically an open-ended box structure containing a water-cooled inner lining fabricated from a high purity copper alloy. The box can come in many shapes and sizes in order to cast different semis: blooms, billets, round beam blanks, slabs and thin slabs. A thin film of lubricating oil or of lubricating flux is interposed between the mould and the hot liquid phase to prevent its direct contact with the mould, which could potentially endanger and damage the mould itself (Fig. 1b). The surface of the copper mould coming in contact with the hot liquid metal is often plated with chromium or nickel to provide a harder working surface and to avoid copper pick-up on the surface of the cast strand, which can facilitate the development of the surface cracks on the cast product.

Maintaining a reliable, crack-free mould within close dimensional tolerances is also crucial for safety and productivity. Thus, studies [3–7] have been undertaken to better understand the complex thermal and mechanical behaviour of the mould. An extreme temperature gradient takes place across the copper plates and this causes geometrical distortions of the mould; moreover, long hours of operation at high temperatures generates creep. This resultant creep is also associated with a thermal fatigue phenomenon, which is caused by the many room temperature heating and cooling cycles undergone by the mould during the initial and final transitory of the casting sequence [3]. Some authors have attempted to simulate this

* Corresponding author. Tel.: +39 (0)2 2399 8662; fax: +39 (0)2 2399 8644.
E-mail address: silvia.barella@polimi.it (S. Barella).

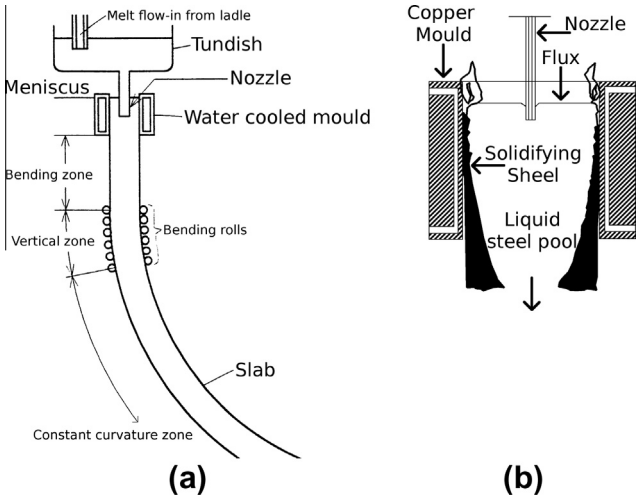

Fig. 1. Sketch of continuous casting machine (a) and mould detail (b) [1].

mechanical behaviour and to predict the potential damage to thin slag-mould systems [4,5] in order to better understand the role played by the machine dynamics in the mould damage process. In addition, friction phenomena could potentially occur between the strand and the mould. Friction between the solidifying steel and the mould is basically sliding (with a small fraction of sticky friction) [8]. These damages could end up having catastrophic consequences. At present, both metallic and ceramic plating are available [9,10]: the latter allows for an increased mould lifespan but it is not widely used due to its cost and low thermal exchange. To the contrary, metallic plating is either nickel or chromium-based. Despite its brittleness and low wear resistance, chromium is the most used metallic element in mould plating. The present study aims at illustrating the failure analysis of a copper liner, with the analysed component being a square mould made of work-hardened pure copper. The square side measures 150 mm and the mould is 1000 mm high. This particular mould was used in a continuous casting machine to produce squared billets and is only one example of the 75 different moulds affected by the same damage phenomenon.

2. Experimental procedure

Fig. 2 shows the mould under investigation. The working mould face had considerable damage in the meniscus region. After an extensive visual examination, the mould was cut into different samples in order to carry out SEM (scanning electron microscope) examination of the damaged surface. The SEM was equipped with an EDS (energy dispersive spectroscopy) probe that was used to perform local chemical analyses. Metallographic analyses were performed to characterize the mould microstructure. These analyses were realized by optical microscopy and SEM. All of the samples were prepared by grinding and polishing. Micro-etching was performed by means of an HCl solution (50 ml HCl, 5 g $FeCl_3$, 100 ml water) applied for 10 s [11]. Micro-hardness Vickers tests were performed with a 300 g load and an indentation time of 15 s.

3. Results and discussion

The examined mould showed significant damage approximately 110 mm from the mould top, at the meniscus level. This damage was even detectable from the external mould side, where the copper mould assumed a colour typical of high

Fig. 2. Failed square mould.

temperature exposure. The visual examination suggested that the temperature had reached 350 °C (Fig. 2). Furthermore, the inner portion of the mould (coated with chromium) had a non-homogeneous surface.

For the in-depth examination along the width of the mould wall, samples were cut from the mould. On the hot face of the mould, a black strip was detected. Many cracks were also visible in this zone: these cracks were aligned along the mould axis (red arrows in Fig. 3). The black area seemed to be constituted by a layer of iron oxide, obtained at a high temperature. In the sample section, a 20 mm eroded region was detectable on the entire surface. The groove was deeper than the chromium plate and this indicated that it was not only due to the chromium wear but also due to the copper erosion as a result of steel percolation through the crack.

A number of samples were grinded and polished in order to obtain a profile of the damaged region. In Fig. 4 the optical-microscope mosaic is reported. During this observation the chromium plate thickness and the groove depth were measured. The chromium plate was approximately 100 μm thick and the dip was 0.96 mm deep (Fig. 4). In this section many cracks were detected: the origin of the cracks was localized on the damaged surface and then the cracks propagated into the thickness.

The SEM analysis was performed on the damaged surface to detect its chemical composition. Investigations were performed on both the damaged surface and the undamaged zone. At high magnification, the undamaged zone aspect (Fig. 5a) was typical of a chromium plate, but some cracks were detectable. These cracks were typical of the chromium deposition process and had been exaggerated by the thermal stress created by the steel casting working conditions [12,13]. In particular the hardness and, as a result, resistance to erosion were decreased. This erosion could potentially cause the complete depletion of the coating. Fig. 5b–d show the damaged area, where the chromium plating is completely removed and the surface aspect is rough.

The EDS analysis referring to the pictures in Fig. 5 are reported in Table 1.

According to the chemical composition analysis (Table 1) the chromium plating was intact in the upper part of the mould (undamaged zone), because it contained a chromium concentration near 100%. The damaged areas were found to be contaminated by many elements contained in the liquid steel, i.e. silicon, manganese and sulphur; moreover, the EDS revealed a significant concentration of zinc in these zones. Zinc is introduced into liquid steel by scrap but it eventually evaporates during melting and secondary steelmaking operations. However, when zinc is dissolved in liquid steel during casting, and plate damage occurs, this element tends to form a brass-type alloy (γ type) within the copper mould. This brass formation reduces the mould toughness along with its physical (thermal and electrical conductivity) and chemical properties (liquid metal corrosion resistance) [14–20].

The SEM analysis performed on the cross section showed a brass layer on the hot face of the mould (Fig. 6 and Table 2). Many cracks were detected but two of these appeared more pronounced. The first was 2.2 mm long (Fig. 7a) and the

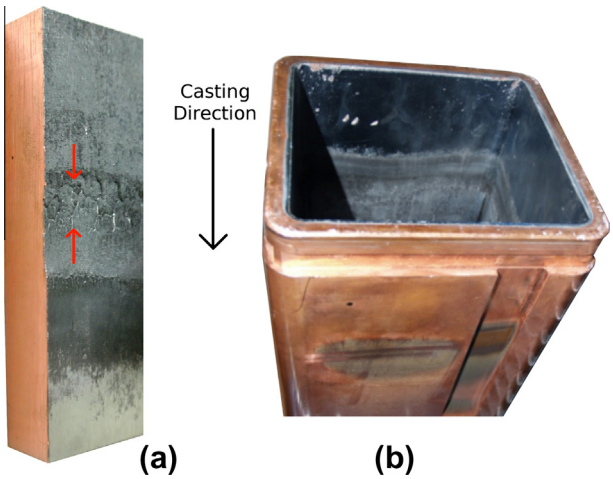

Fig. 3. Damaged mould, the external side assumed a characteristic colour different from its original featuring the entire mould (a) and damaged inner mould side featured by chromium plate removal and cracks (b). (For interpretation of the references to colour in this figure legend, the reader is referred to the web version of this article.)

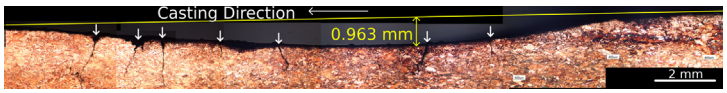

Fig. 4. Mould cross section: measure of the damaged zone (magnification 25×). With arrows indicate cracks.

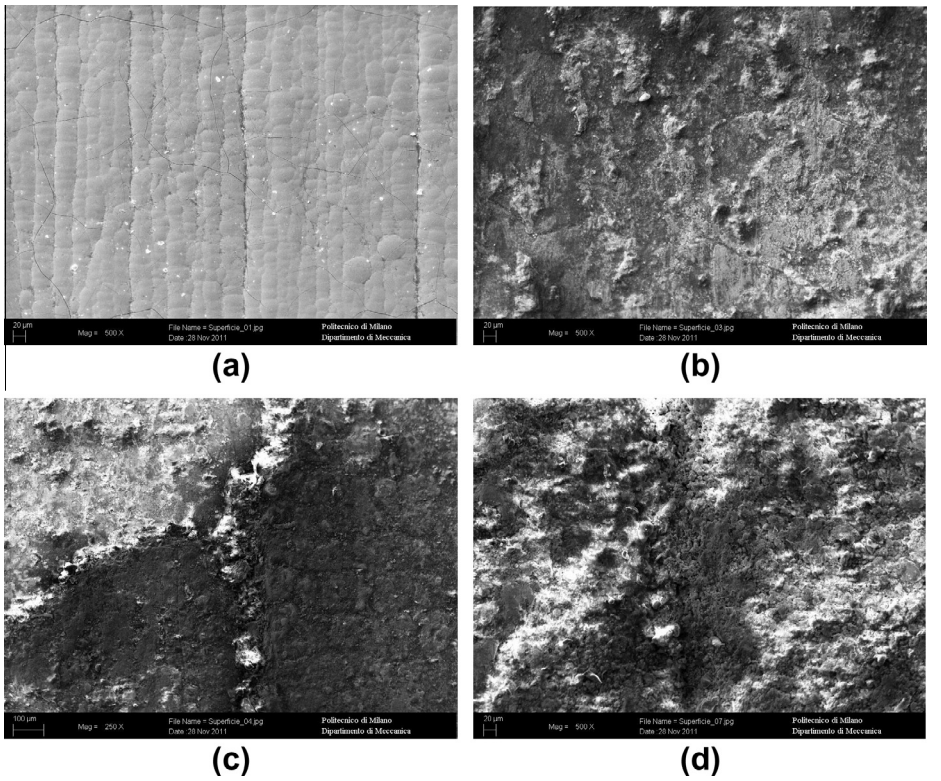

Fig. 5. SEM investigation on undamaged (a) and damaged zones (b–d).

Table 1
SEM–EDS characterization carried out on the pictures represented in Fig. 5.

wt%	O	F	Si	S	Cr	Mn	Fe	Cu	Zn	Sn	Pb
Picture											
(a)					99.56			0.44			
(b)	18.45	2.03	0.85	3.85	13.44	14.11	1.68		43.09		
(c)	11.78	1.42	2.01	23.66		19.75	4.70	6.38	20.16	8.92	
(d)	17.45	4.93	1.46	3.98		5.11	2.49	1.35	26.71		27.01

Fig. 6. SEM investigation on the section of the damaged zone.

Table 2
SEM–EDS characterization carried out on the zone represented in Figs. 6–8.

wt%	O	F	Si	S	Cr	Mn	Fe	Cu	Zn	Pb
Picture										
Fig. 6A								35.21	64.44	
Fig. 7(b) A						1.21	95.21	0.93	0.81	
Fig. 7(b) B	1.80						0.56	97.34		
Fig. 7(b) C	10.78	5.23		18.94		4.87	0.97	13.01	44.33	
Fig. 7(b) D	8.96					1.35	0.82	4.58	7.65	75.33
Fig. 8A					100					
Fig. 8B								39.57	60.43	
Fig. 8C								100		

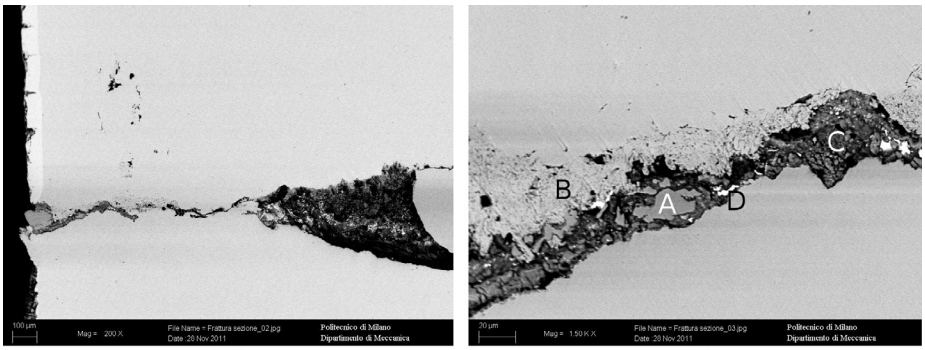

Fig. 7. SEM investigation on the section of the damaged zone, crack detail.

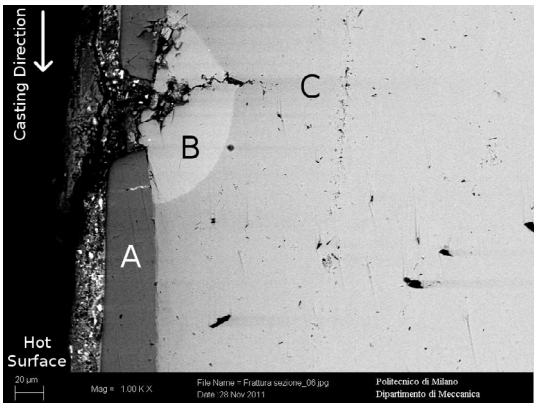

Fig. 8. SEM investigation on the section of the damaged zone, crack detail.

surrounding areas seemed recrystallized (Fig. 7b). In addition to zinc, many other residual impurities (i.e. Fe, S, and Pb) were detected in the crack due to the liquid steel infiltration (Table 2).

The crack shown in Fig. 8 displayed an interesting brass layer formation due to chromium plating damage, which was a consequence of the zinc diffusion in the copper matrix. The variation of the concentration profile (Fig. 9) provided for good identification of the layer's chemical composition in the undamaged (a) and damaged zones (b).

Some detachment of the chromium coating was also detected in the form of secondary cracking. Most probably, this was due to a change in interface conditions that decreased the chromium adhesion.

The mould microstructure was analysed, after the application of an appropriate etching, both on the undamaged and damaged zones (Fig. 10).

Fig. 10a displays the microstructure of a sample taken far from the damaged zone: the average size of the grain is roughly 100 μm. Many other observations were performed on the sample obtained from the damaged zone (Fig. 10b). The grains were finer than in the undamaged zone and the cracks propagated along the grain boundaries (intergranular fracture).

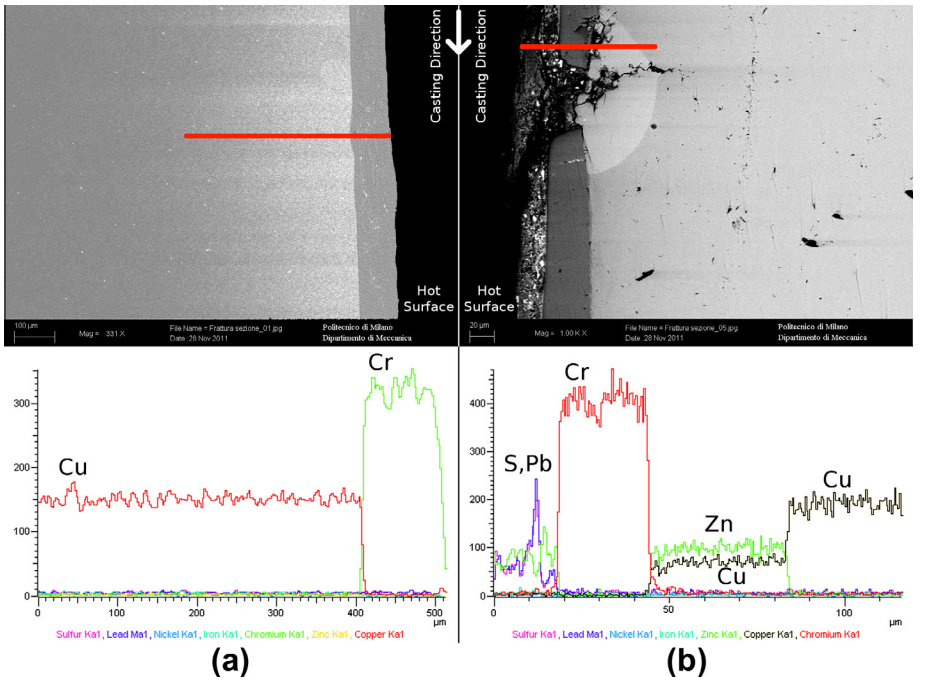

Fig. 9. Elements concentration profiles (a) on the undamaged and (b) the damaged zones (linescan were performed on the red line). (For interpretation of the references to colour in this figure legend, the reader is referred to the web version of this article.)

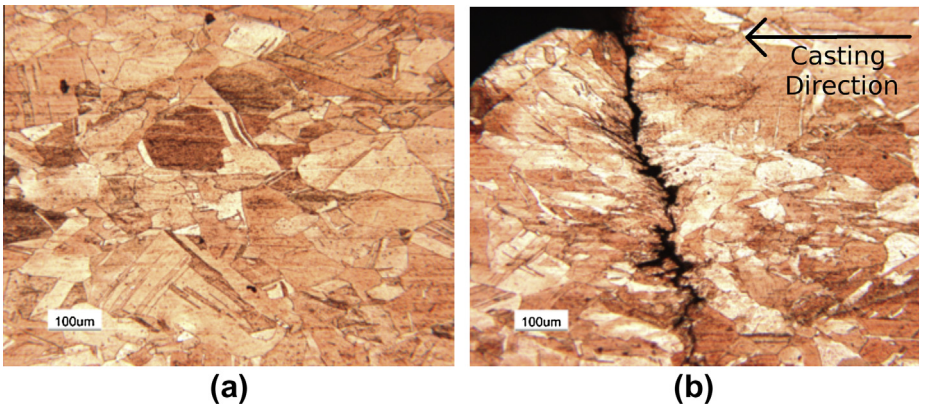

Fig. 10. Microstructure on (a) the mould central zone and (b) on the damaged zone.

The microstructure seemed to have undergone a recrystallization process near the crack because of the small grain size [21]. Moreover, in some areas, the copper appeared melted due its contact with the liquid steel.

The grain size measurement (ASTM E112-96 (2004)) confirmed the recrystallization hypothesis: the G number was approximately 5.2 in the undamaged zones and roughly 7.1 in the damaged areas.

Finally, micro-hardness tests allowed for a better understanding of the extension of the thermal-affected mould zone due to the liquid steel infiltration (Fig. 11). The area near the damage showed the lowest hardness number (80–90-HV) due to a static recrystallization phenomenon followed by the grain growth. Instead, the outer part of the mould showed the typical hardness value for this kind of work-hardened copper (115–130 HV) [17,19]. Between these two regions the heat-affected zone could be identified as the zone characterized by intermediate hardness numbers (100–115 HV). This indicated that the recrystallization phenomena had taken place. The work hardened material retained energy in the form of lattice defects and the driving force for recrystallization was this stored energy. The heat given off from the high temperatures of the liquid phase provided the thermal activation energy needed to transform the material to a lower energy state, through a diffusion process. As the internal lattice strains were relieved during annealing, the hardness decreased [22].

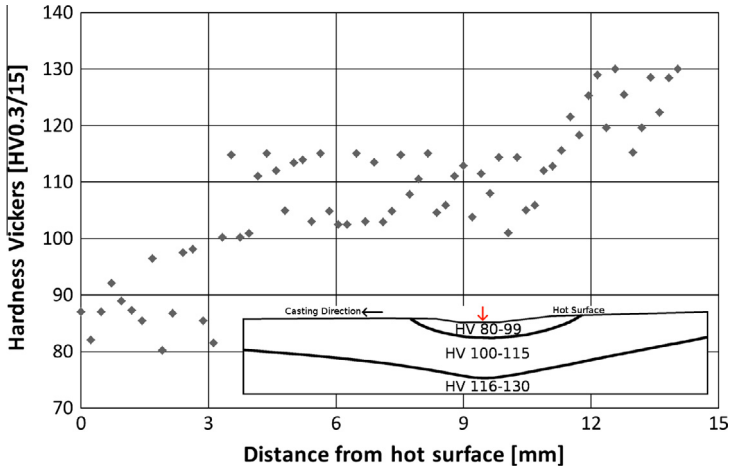

Fig. 11. Micro-hardness profile along the cross section of the mould near the damaged zone and schematic representation of the micro-hardness trend. Red arrows indicate the initial site of the profile.

4. Conclusion

The failure analysis conducted on the casting machine mould led to a better understanding of the failure mechanism. First, the chromium coating was naturally cracked due to the deposition process, and these cracks were able to propagate thanks to the thermal stresses caused by the mould's working conditions. In addition, the high working temperatures led to an increase in chromium erosion. With the cracks having penetrated the entire plating thickness, the liquid steel remained in contact with the copper. The zinc within the liquid steel diffused in the copper forming a brass alloy with a high zinc content. Both the brass brittleness and the recrystallization phenomenon, characterized by copper softening, promoted the crack propagation.

The observed damage is very dangerous because it can cause the continuous casting machines to breakdown. For this reason, Zn concentration of the cast steels must be reduced in order to avoid this detrimental phenomenon, given that intrinsic chromium cracking, thermal stresses and the related coating erosion could not be avoided.

References

[1] Mapelli C, Nicodemi W. Siderurgia. 2nd ed. Milano: AIM; 2011.
[2] Irwing WR. Continuous casting of steel. London: The Institute of Materials; 1993.
[3] Thomas BG, Li G, Moitra A, Habing D. Analysis of thermal and mechanical behavior of copper molds during continuous casting of steel slabs, 80th steelmaking conference, (Chicago, IL, April 13–16, 1997), ISS Herty Award Page 1 of 19.
[4] O'connor TG, Dantzig JA. Modeling the thin-slab continuous-casting mold. Metall Mater Trans B 1994;25B:443.
[5] Park JK, Thomas BG, Samarasekera IV, Yoon US. Thermal and mechanical behavior of copper molds during thin-slab casting (II): mold crack formation. Metall Mater Trans B 2002;33B:437.
[6] Gravemann H. Mould tubes with improved service life for continuous casting of steel. Continuous Casting'85. London: The Institute of Metals; 1985. p. 201–209.
[7] Li M, Stubbins JF. Creep fatigue behavior in high strength copper alloys. J ASTM Int 2005;2.
[8] Sanz A. Tribological behavior of coatings for continuous casting of steel. Surf Coat Technol 2001;147:55–64.
[9] Pandey JC, Raj Manish, Mishra Rajesh, Tripathy VK, Bandyopadhya N. Failure of nickel coating on a copper mold of a slab caster. J Fail Anal Prevent 2008;8:3–11.
[10] Brower JK, Rapp KD. Advanced alternative coatings for mold copper liners. Michael J. Powers, P.E, Iron and Steel Technology. July 2006.
[11] AA VV. ASM metals handbook, vol. 9. 9th ed. Material Park, Ohio: The Materials International Society; 1995.
[12] Hadavia SMM, Abdollah-Zadehb A, Jamshidic MS. The effect of thermal fatigue on the hardness of hard chromium electroplatings. J Mater Process Technol 2004;147:385–8.
[13] AA VV. ASM handbook, vol. 5. Material Park, Ohio: The Materials International Society; 1995 [1994].
[14] Carter GF. Principles of physical and chemical metallurgy. Material Park, Ohio: The Materials International Society; 1979.
[15] Clark DS, Varney FR. Physical metallurgy for engineers. New York: D. Van Nostrand Company Inc.; 1953.
[16] Abbaschian R, Abbashian L, Reed-Hill RE. Physical metallurgy principles. 4th ed. Stamford: Cengage Learning; 2011.
[17] Nicodemi W. Acciai e leghe non ferrose. 2nd ed. Milano: Zanichelli; 2008.
[18] Loconsolo V, Nobili L. Il manuale degli ottoni. Milano: Consedit; 1995.
[19] AA VV. Properties and selection: nonferrous alloys and special-purpose materials, vol. 2. 10th ed. Material Park, Ohio: The Materials International Society; 1990.
[20] AA VV. Alloy phase diagrams, vol. 3. Material Park, Ohio: The Materials International Society; 1990.
[21] Humphreys FJ, Hatherly M. Recrystallization and related annealing phenomena. 2nd ed. Oxford: Elsevier; 2004.
[22] Campbell FC. Elements of metallurgy and engineering alloys. Material Park, Ohio: The Materials International Society; 2008.